Pergamon

SCIENCE DIRECT®

Bioorganic & Medicinal Chemistry Letters 13 (2003) 2955–2960

BIOORGANIC & MEDICINAL CHEMISTRY LETTERS

Cyclin-Dependent Kinase 4 Inhibitors as a Treatment for Cancer. Part 1: Identification and Optimisation of Substituted 4,6-Bis Anilino Pyrimidines

John F. Beattie, Gloria A. Breault,* Rebecca P. A. Ellston, Stephen Green, Philip J. Jewsbury, Catherine J. Midgley, Russell T. Naven, Claire A. Minshull, Richard A. Pauptit, Julie A. Tucker and J. Elizabeth Pease*

AstraZeneca, Alderley Park, Macclesfield, Cheshire SK10 4TG, UK

Revised 19 September 2002; accepted 20 December 2002

Abstract—Using a high-throughput screening campaign, we identified the 4,6-bis anilino pyrimidines as inhibitors of the cyclin-dependent kinase, CDK4. Herein we describe the further chemical modification and use of X-ray crystallography to develop potent and selective in vitro inhibitors of CDK4.

Cancer has long been recognized as a disease of aberrant cellular proliferation. Traditional cancer therapies aim to exploit the proliferative machinery, for example, DNA replication or chromosome segregation. As such, they demonstrate only partial selectivity for tumour cells compared with normal proliferating tissues such as the gut and bone marrow. More recently, many of the proteins regulating entry into, progression through and exit from the cell cycle, have been identified and their roles elucidated.[1] In particular, it is now recognised that many of these proteins are themselves mutated, deleted or over-expressed in cancer leading to the deregulated growth of the tumour cell. Such proteins, therefore, represent potential targets to develop more selective agents that may have an improved therapeutic margin in the clinic.

The cyclin-dependent kinases (CDKs) are especially important in controlling entry into and progression through the cell cycle.[1] They are a family of serine/threonine kinases whose activity is regulated at several levels. The binding of each CDK to a specific cyclin partner protein is required for activity. The synthesis and degradation of cyclins is tightly controlled such that their level fluctuates during the cell cycle. It is these fluctuating levels of the cyclin that cause first one, and then another member of the CDK family to become active during cell cycle progression. Inhibitory proteins, such as members of the p16INK4A family or the p21CIP/p27KIP family, also regulate CDK activity and these inhibitors must be either sequestered or destroyed to allow the CDK enzyme to become fully activated. As cells respond to the presence of mitogens, the level of cyclin D1 increases and eventually triggers the activation of CDK4 and CDK6. These kinases phosphorylate the retinoblastoma tumour suppressor protein pRb thereby abrogating its inhibition of members of the E2F family of transcription factors. This then triggers a programme of gene expression that results in entry into the S phase of the cell cycle.

There are now many examples where tumours contain multiple copies of the cyclin D1 gene or express abnormally high levels of the protein.[2] Similarly, many tumours have been described that contain mutations, deletions or silencing of the p16 or the pRb gene.[3,4] Finally, mutations of CDK4 itself have been described within melanoma patients, where the region of the enzyme that binds p16 has been mutated making the enzyme resistant to inhibition.[5] Together, these findings imply that the deregulation of the pRb pathway, and CDK4, is important in cancer progression. The inhibition of CDK4 may therefore be a valuable approach to treat tumours that have lost the natural CDK4 inhibitor, p16. In this respect, it is interesting to note that

*Corresponding author. E-mail: j.elizabeth.pease@astrazeneca.com

0960-894X/03/$ - see front matter © 2003 Elsevier Ltd. All rights reserved.
doi:10.1016/S0960-894X(03)00202-6

adenovirus vectors expressing p16 have been shown to induce tumour regression in animal models.[6]

A number of groups have identified CDK inhibitors.[7–18] In this paper, we describe a series of novel, potent inhibitors of CDK4 with selectivity against CDK2. Such compounds may prove valuable in treating tumours with deregulated CDK4 such as those lacking p16.

A high-throughput screen of the AstraZeneca compound collection using an in vitro scintillation proximity assay (SPA) for measuring incorporation of [γ-33-P]-adenosine triphosphate into GST-Rb,[18] identified the 4,6-bis anilino pyrimidine **1** as an inhibitor of CDK4 (IC_{50} 15 μM) possessing some selectivity against CDK2 (IC_{50} 93 μM). This prompted us to initiate chemistry to explore the activity of this class of compounds.

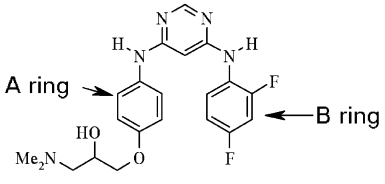

1

Our initial goals were to improve potency, demonstrate evidence of SAR and, ideally, generate compounds with adequate solubility to allow protein ligand X-ray crystallography studies. The synthetic route to **1** and related compounds is illustrated in Scheme 1. Reaction of 4,6-dichloropyrimidine with 4-hydroxyaniline gave the monochloro intermediate **1-1**. This intermediate was treated with the appropriate aniline to introduce ring B resulting in intermediate **1-2**. The phenol was then alkylated with epibromohydrin followed by ring opening of the epoxide with dimethyl amine resulting in the final compound.

One aspect of the work concentrated on evaluating the effect of substituents in ring B, such as the 2-substituents illustrated in Table 1. The unsubstituted compound **2** was less potent than the original hit but still retained some activity and selectivity. Within this limited sub-series it was evident that a range of substituents are tolerated with the 2-bromo **7** and 2- nitro **9** derivatives being the most potent. However, the SAR was difficult to interpret. Later, it became apparent from the crystal structures that the B-ring in this series takes up a range of orientations making interpretation of activity trends difficult. The 2-chloro **6** and 2-methyl **3** substituents were of interest due to the increased potency. These substituents along with the 2-fluoro **5** were chosen for further investigation because the accessibility of polyfunctionalised anilines would allow the work to progress to disubstitution of ring B, which we believed would result in enhancements in potency.

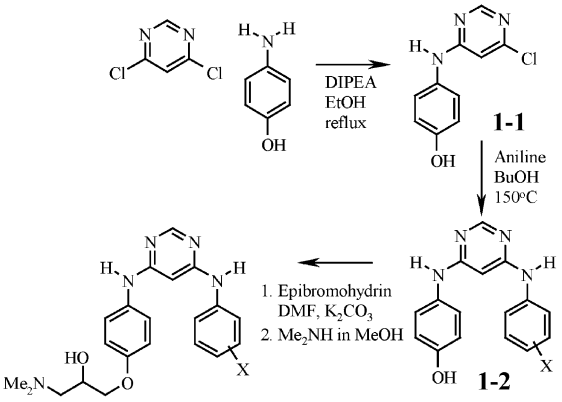

Scheme 1. Synthesis of 4,6-bis anilino pyrimidines.

Table 1. Structures and enzyme activity for 4,6-bis anilino pyrimidines

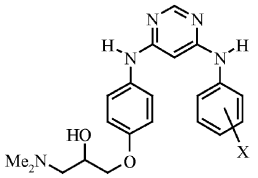

Compd	CDK4 IC_{50} (μM)[a]	CDK2 IC_{50} (μM)[a]	X
1	15	93	2,4-F_2
2	33	>100	H
3	8	39	2-Me
4	18	24	2-*i*Pr
5	27	>100	2-F
6	8	95	2-Cl
7	4	28	2-Br
8	23	85	2-OMe
9	2	25	2-NO_2

[a]Values are means of at least two determinations. The assay-to-assay variation was generally ±2-fold based on the results of a standard compound.

Among the disubstituted derivatives that were prepared, three were of particular interest (Table 2). The 2,5-dichloro **10** demonstrated that enhanced potency could be achieved. The 2,6-difluoro **11** and the 2-fluoro, 5-trifluoromethyl **12** were also significant as they combined moderate potency with suitable solubility for structural studies[19] and led to protein–ligand crystal structures

Table 2. Structures and enzyme activity for disubstituted 4,6-bis-anilino pyrimides

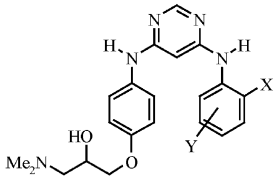

Compd	CDK4 IC_{50} (μM)[a]	CDK2 IC_{50} (μM)[a]	X	Y
10	1	22	2-Cl	5-Cl
11	9	38	2-F	6-F
12	6	35	2-F	5-CF_3

[a]Values are means of at least two determinations. The assay-to-assay variation was generally ±2-fold based on the results of a standard compound.

that allowed us to improve our understanding of how the compounds were binding.

In these structural studies, inactive CDK2 monomer was used as a structural surrogate for the CDK4 target. This approach is convenient since the crystal structure of CDK2 is known,[20] and the crystals are particularly robust, often diffract to high resolution and can readily be soaked in inhibitor solutions enabling rapid experimental support for molecular design strategies. The binding conformations obtained with CDK2 were interpreted assuming they were relevant to the true CDK4 target. While the use of these structural surrogates for molecular design will be limited where the details of the protein–ligand interactions differ, our studies of a range of inhibitor series bound to a range of kinase targets indicate that, in general, the bioactive conformation of the series is conserved, even between kinases with distant sequence relationships (unpublished work).

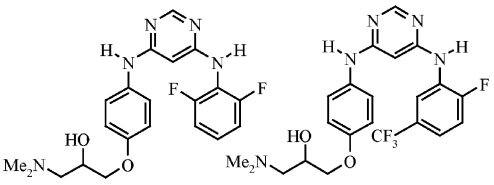

11 **12**

Crystal structures[19] of CDK2 complexed with **11** and **12** revealed the binding mode of this series: the pyrimidine N1 acts as a hydrogen bond acceptor with the 6-aniline NH acting as a hydrogen bond donor (Fig. 1). The former interaction, with the Leu 83 amide NH, is also seen in the CDK2–ATP complex;[20] the second interaction is with the Leu 83 amide carbonyl oxygen. Both these interactions are consistent with the accepted kinase purine-mimetic pharmacophore: a central hydrogen bond acceptor flanked by two hydrogen bond donating groups. Purine-mimetic kinase inhibitors reported to date have one, two or all three of these interactions.[20,33]

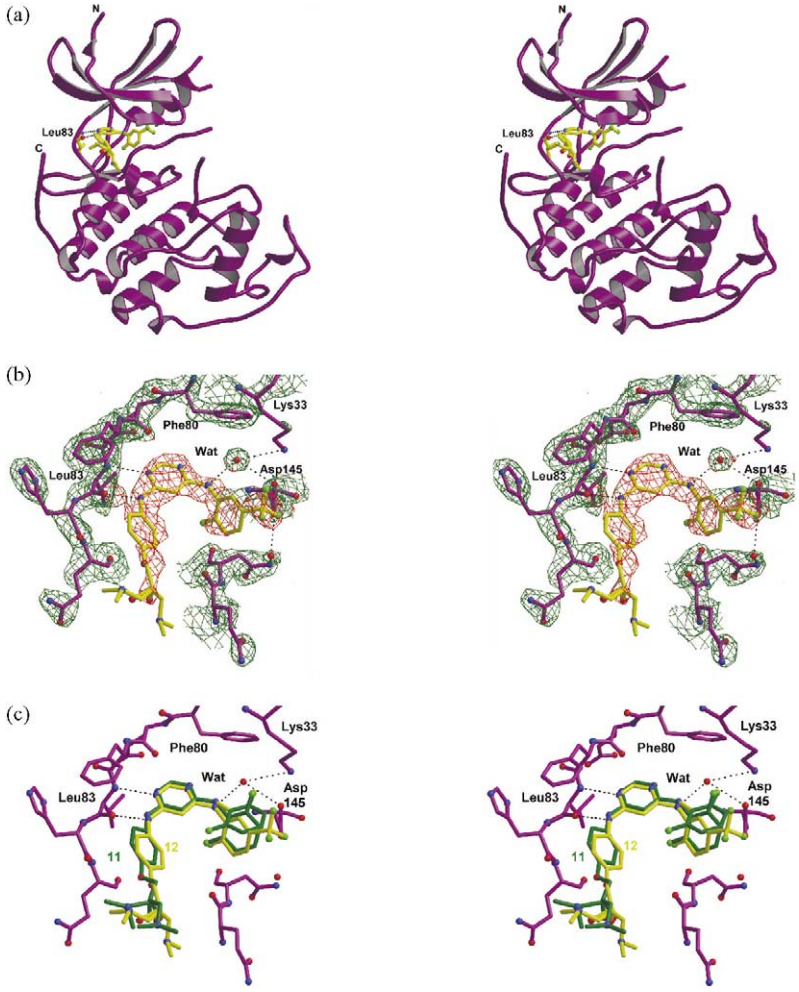

Figure 1. Crystal structures of CDK2 complexed with **11** and **12**: (a) ribbon diagram showing the location of **12** in the purine pocket between the N-terminal and C-terminal domains of CDK2; (b) final 2Fo-Fc electron density for the protein (green, 1.3σ level) and for the inhibitor **12** (red, 1.3σ level) calculated in the vicinity of the ATP-binding site of CDK2. The trifluoromethyl substituent is clearly visible defining the orientation of ring B. The bridging water molecule between the 4-anilino NH and Asp145 is well defined, whereas Lys33 becomes mobile. There is typically very little density for the solubilising group (which is modelled as a racemic mixture) indicating this part of the inhibitor is disordered; (c) superposition of the binding modes of **11** and **12**. The racemic solubilising group is also poorly defined in **11**. Ring B in **11** adopts two conformations: in both, one of the fluoro substituents displaces the bridging water. In both, the orientation is different to **12**. The figures were prepared using Bobscript and Raster3D.[30–32]

Given the symmetry of the 4,6-bis anilino pyrimidine substructure, the orientation within the binding site is determined by the substitution pattern on the aniline rings. In this series, ring A was *para*-substituted by a 'solubilising' group, and is oriented towards solvent at the edge of the ATP binding site. Ring B, with lipophilic substituents, lies inside the binding site. Comparison of the two structures, however, revealed that while the position of the hydrogen bonding groups was conserved, the orientation of ring B was variable. In particular, in the complex with **12** a water molecule bridges between the 4-aniline NH and Asp145, disrupting the Lys33-Asp145 salt bridge. This water molecule is displaced by ring B in the complex with **11**, with the 2-fluoro near the water position (Fig. 1).

Since these initial structures indicated that this water molecule could be readily displaced, and that ring B could occupy a range of orientations, we decided to synthesise compounds that could exploit the space available in both ring B binding modes simultaneously. By *N*-alkylating the 4-aniline NH, it was proposed that ring B would orientate in a manner similar to that seen in the complex with **12** (Fig. 1), and the *N*-alkyl substituent would displace the water molecule.

As earlier work had suggested the 2,5-dichloro substitution pattern to be potent we decided to investigate the effects of *N*-alkylation within this series. The 4,6-dichloropyrimidine was reacted with 2,5-dichloroaniline followed by reaction with 4-hydroxyaniline. The phenol was then reacted with epibromohydrin. The resulting epoxide **2-1** acted as a protecting group during the alkylation. The aniline nitrogen was then alkylated and the epoxide opened with dimethyl amine to yield the final product (Scheme 2).

A selection of compounds that were alkylated on the 4-aniline nitrogen is shown in Table 3. In general, the potency of the compounds improved with alkylation. By far the most advantageous *N*-substituent was cyanomethyl, **13** that showed a 20-fold improvement in potency over the unsubsituted, **10**. Lengthening of the carbon chain by one **14** reduced the activity by an order of magnitude. The cyano group appeared to make specific interactions, as changing to an acetylene group, **15**, resulted in a 10-fold decrease in potency, despite an increase in the lipophilicity. Once the *N*-substituent became bulky **16**, potency was substantially reduced, however, favourable effects on selectivity versus CDK2 were still observed.

The structure of an analogue of **13**, the 2-bromo, 4-methyl **17** (CDK4 IC_{50} 0.1 μM, CDK2 IC_{50} 3 μM) bound to CDK2 was solved revealing a binding mode consistent with the design hypothesis: the B-ring orientation was similar to that found for **12** but with the methylenenitrile displacing the bridging water. The nitrile C lies within 1.3 Å of the water, consistent with a drop of activity on extending the alkyl chain, **14** (Fig. 2). The nitrile triple bond is stacked against the π cloud of the Phe80 side chain, with its polarity complimentary to the local electrostatic potential caused by the Lys33 side chain. The loss of this electrostatic complimentarity may account for the drop in activity found for **15**. Bulky alkyl chains **16** can no longer be accommodated by this binding mode, presumably causing an alternative orientation with consequent loss in activity.

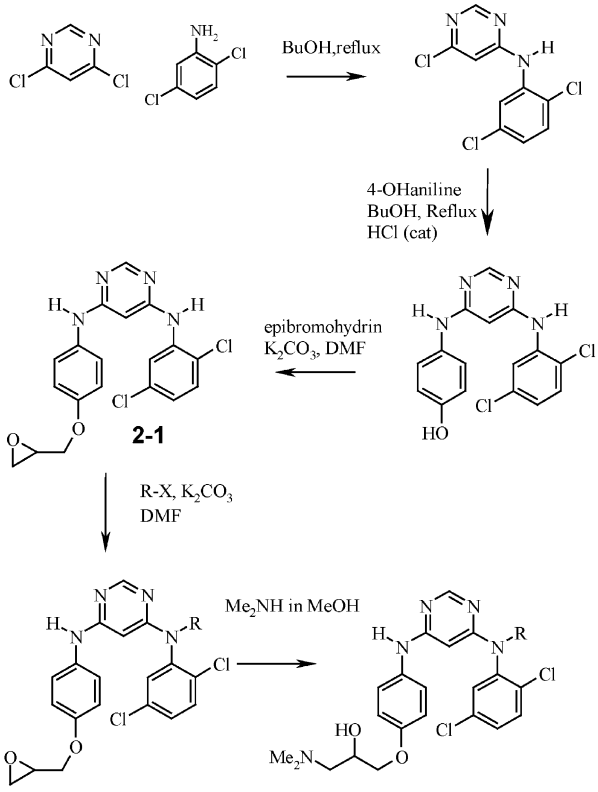

Scheme 2. Synthesis of alkylated 4,6-bis anilino pyrimidines.

Table 3. Structures and enzyme activity for alkylated 4,6-bis anilino pyrimides

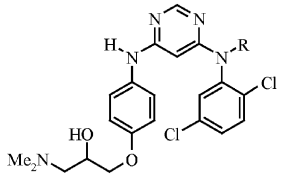

Compd	CDK4 IC_{50} (μM)[a]	CDK2 IC_{50} (μM)[a]	R
10	1	22	H
13	0.05	1	CH_2CN
14	0.5	5	CH_2CH_2CN
15	0.8	19	CH_2CCH
16	5	>100	CH_2Ph

[a]Values are means of at least two determinations. The assay-to-assay variation was generally ±2-fold based on the results of a standard compound.

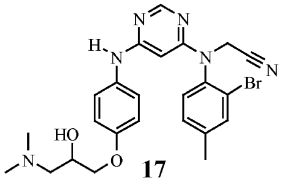

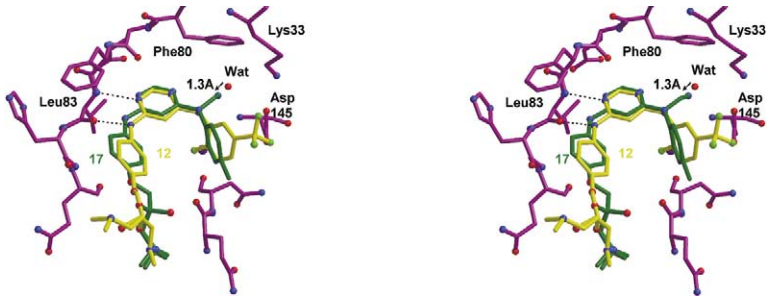

Figure 2. Superposition of the binding modes of **12** and **17**. The nitrile C lies within 1.3 Å of the position occupied by the bridging water molecule in the complex between CDK2 and **12**. The racemic solubilising group is also poorly defined in **17**. Ring B in **17** adopts an orientation similar to **12**. The figures were prepared using Bobscript and Raster3D.[30–32]

In conclusion, we identified a novel series of 4,6-bis anilino pyrimidines as CDK4 inhibitors using high throughput screening. Through modifications to ring B an increase in potency (10-fold) and improved solubility were achieved, allowing protein–ligand structures (with CDK2) to be obtained. These revealed that two binding modes of the compounds are possible and the insight provided by the structural work led us to introduce specific substituents on the 4-aniline NH. The resulting 2,5-disubstituted *N*-alkylated 4,6-bis anilino pyrimidines represent highly potent and selective inhibitors of CDK4 that are the subject of further investigations.

Acknowledgements

We are grateful for the excellent support we have received from Michael Block and would also like to thank Sandra Oakes for repeat enzyme measurements.

References and Notes

1. Sherr, C. J. *Science* **1996**, *274*, 1672.
2. Barnes, D. M.; Gillet, C. E. *Breast Cancer Res. Treat*. **1998**, *52*, 1.
3. Roussel, M. F. *Oncogene* **1999**, *18*, 5311.
4. Nevins, J. R. *Hum. Mol. Genet*. **2001**, *10*, 699.
5. Tsao, H.; Benoit, E.; Sober, A. J.; Thiele, C.; Haluska, F. G. *Cancer Res*. **1998**, *58*, 109.
6. Frizelle, S. P.; Grim, J.; Zhou, J.; Gupta, P.; Curiel, D. T.; Geradts, J.; Kratzke, R. A. *Oncogene* **1998**, *16*, 3087.
7. Webster, K. R.; Kimball, S. D. *Emerg. Drugs* **2000**, *5*, 45.
8. Kimball, S. D.; Webster, K. R. In *Annual Reports in Medicinal Chemistry*; Doherty, A. M., Ed.; Academic: San Diego, 2001; Vol. 36, p 139 and references therein.
9. Ikuta, M.; Kamata, K.; Fukasawa, K.; Honma, T.; Machida, T.; Hirai, H.; Suzuki-Takahashi, I.; Hayama, T.; Nishimura, S. *J. Biol. Chem*. **2001**, *276*, 27548.
10. Carini, D. J.; Kaltenbach, R. F.; Liu, J.; Benfield, P. A.; Boylan, J.; Boisclair, M.; Brizuela, L.; Burton, C. R.; Cox, S.; Grafstrom, R.; Harrison, B. A.; Harrison, K.; Akamike, E.; Markwalder, J. A.; Nakano, Y.; Seitz, S. P.; Sharp, D. M.; Trainor, G. L.; Sielecki, T. M. *Bioorg. Med. Chem. Lett*. **2001**, *11*, 2209.
11. Honma, T.; Hayashi, K.; Aoyama, T.; Hashimoto, N.; Machida, T.; Fukasawa, K.; Iwama, T.; Ikeura, C.; Suzuki-Takahashi, I. *J. Med. Chem*. **2001**, *44*, 4615.
12. Fry, D. W.; Bedford, D. C.; Harvey, P. H.; Fritsch, A.; Keller, P. R.; Wu, Z.; Dobrusin, E.; Leopold, W. R.; Fattaey, A.; Garrett, M. D. *J. Biol. Chem*. **2001**, *276*, 16617.
13. Soni, R.; O'Reilly, T.; Furet, P.; Muller, L.; Stephan, C.; Zumstein-Mecker, S.; Fretz, H.; Fabbro, D.; Chaudhuri, B. *J. Natl. Cancer Inst*. **2001**, *93*, 436.
14. Honma, T.; Yoshizumi, T.; Hashimoto, N.; Hayashi, K.; Kawanishi, N.; Fukasawa, K.; Takaki, T.; Ikeura, C.; Ikuta, M.; Suzuki-Takahashi, I.; Takashi, H.; Nishimura, S.; Morishima, H. *J. Med. Chem*. **2001**, *44*, 4628.
15. Soni, R.; Muller, L.; Furet, P.; Schoepfer, J.; Stephan, C.; Zumstein-Mecker, S.; Fretz, H.; Chaudhuri, B. *Biochem. Biophys. Res. Commun*. **2000**, *275*, 877.
16. Jeong, H.-W.; Kim, M.-R.; Son, K.-H.; Young Han, M.; Ha, J.-H.; Garnier, M.; Meijer, L.; Kwon, B.-M. *Bioorg. Med. Chem. Lett*. **2000**, *10*, 1819.
17. Ryu, C.-K.; Kang, H.-Y.; Lee, S. K.; Nam, K. A.; Hong, C. Y.; Ko, W.-G.; Lee, B.-H. *Bioorg. Med. Chem. Lett*. **2000**, *10*, 461.
18. Breault, G. A., Pease, J. E. PCT Int. Application WO 0012485 A1 20000309.
19. Protein and crystals were obtained according to established procedures[21,22] Diffraction data were collected on beamline 9.6 at SRS, Daresbury, at 100 K. Data processing, data reduction and structure solution by molecular replacement were carried out using programs from the CCP4 suite.[23] Compounds **11**, **12**, and **17** were modelled as racemic mixtures of the chiral alcohol using InsightII,[24] and modelled into electron density using QUANTA.[25] The protein complex model was refined using CNX[26] and Buster,[27] and final structures[28,29,30] have been deposited in the Protein Data Bank with deposition codes 1h00, 1h06 and 1h07 together with structure factors and detailed experimental conditions.
20. Schulze-Gahmen, U.; DeBondt, H. L.; Kim, S.-H. *J. Med. Chem*. **1996**, *39*, 4540.
21. Lawrie, A. M.; Noble, M. E.; Tunnah, P.; Brown, N. R.; Johnson, L. N.; Endicott, J. A. *Nat. Struct. Biol*. **1997**, *4*, 796.
22. Legraverend, M.; Tunnah, P.; Noble, M.; Ducrot, P.; Ludwig, O.; Grierson, D. S.; Leost, M.; Meijer, L.; Endicott, J. *J. Med. Chem*. **2000**, *43*, 1282.
23. CCP4 *Acta Crystallogr*. **1994**, *D50*, 760.
24. InsightII, Accelrys.
25. Quanta2000, Accelrys.
26. CNX version 2000.1, Accelrys.
27. Buster, Global Phasing.
28. Crystallographic statistics for **11** are: space group $P2_12_12_1$, unit cell 54.3, 72.2, 72.1 Å, resolution 1.6 Å, 35229 unique reflections from 106,279 observations give 93.6% completeness with $R_{merge} = 3.6\%$ and mean $I/\sigma(I)$ of 21.The final model containing 2175 protein, 200 water and 44 inhibitor atoms has an R-factor of 21% (R_{free} using 5% of data is 25%). Mean temperature factor for protein is 26.4 and for ligand is 43.2 $Å^2$.

29. Crystallographic statistics for **12** are: space group P212121, unit cell 54.3, 72.9, 73.8 Å, resolution 2.3 Å, 11954 unique reflections from 30352 observations give 90.6% completeness with $R_{merge} = 7.8\%$ and mean $I/\sigma(I)$ of 13. The final model containing 2181 protein, 88 water and 33 inhibitor atoms has an R-factor of 22% (R_{free} using 5% of data is 26%). Mean temperature factor for protein is 23.5 and for ligand is 46.8 $Å^2$.
30. Crystallographic statistics for **17** are: space group P212121, unit cell 53.3, 71.5, 72.6 Å, resolution 1.85 Å, 21,455 unique reflections from 53,065 observations give 87.7% completeness with $R_{merge} = 9.6\%$ and mean $I/\sigma(I)$ of 10. The final model containing 2285 protein, 200 water and 39 inhibitor atoms has an R-factor of 21% (R_{free} using 5% of data is 23.5%). Mean temperature factor for protein is 23 and for ligand is 44 $Å^2$.
31. Esnouf, R. *J. Mol. Graph.* **1997**, *156*, 132.
32. Merritt, E. A.; Murphy, M. E. P. *Acta Crustallogr.* **1994**, *D50*, 869.
33. Bacon, D.; Anderson, W. F. *J. Mol. Graph.* **1988**, *6*, 219.